

## Coastal and River Embankment Performance at Cengkareng Drain Estuary Under Compound Hazards Conditions Using HEC-RAS 2D

Athena Hastomo<sup>1,\*</sup>, Evi Anggraheni<sup>1</sup>, Adi Prasetyo<sup>2</sup>, Dwita Sutjiningsih<sup>1</sup>, Mochamad Adhiraga Pratama<sup>1</sup>, Atina Umi Kalsum<sup>3</sup>

<sup>1</sup>Department of Civil and Environmental Engineering, Universitas Indonesia, Depok, INDONESIA

<sup>2</sup>Coastal Engineering Agency, Directorate General of Water Resources, INDONESIA

<sup>3</sup>Water Resources Engineering, Vrije Universiteit Brussel, BELGIUM

\*Corresponding author: [athena.hastomo@ui.ac.id](mailto:athena.hastomo@ui.ac.id)

SUBMITTED 06 March 2023 REVISED 10 May 2023 ACCEPTED 17 June 2023

**ABSTRACT** Jakarta is prone to pluvial, fluvial, and coastal flooding due to its geographical location and topography. In response to this problem, the Indonesian government has implemented several master plans, including the National Capital Integrated Coastal Development (NCICD). This ongoing program encompasses the construction of coastal and river embankment that stretch all over the coast of Jakarta. Since many coastal areas in Jakarta are residential or industrial, evaluating this performance of embankment has become crucial for effective flood management. The findings of this research can also support the development of other locations where NCICD embankment plan and enhance coastal resilience. Therefore, this research assessed the effectiveness of coastal and river embankment at Cengkareng Drain, a vital floodway in Jakarta, during extreme events that occur simultaneously. To simulate flooding events, two-dimensional HEC-RAS features were used to numerically calculate the area and depth of inundation. The simulation required geometry, terrain, land cover, and unsteady flow data. For the flow boundary conditions, a 100-year design rainfall, HHWL (Highest High-Water Level), and 100-year design wave were considered to represent estuary conditions accurately. The simulation result showed that the maximum water level influenced by these factors was +3.145 mMSL, while the planned embankment top elevation was +3.40 mMSL. Furthermore, without the NCICD embankment, the simulation showed an inundation area of 1212.37 ha, which was reduced to 1111.22 ha after their implementation, leading to a decrease of 101.15 ha. This reduction significantly decreases potential damage to property and infrastructure, particularly in densely populated areas. The simulation also showed a reduction of 86.49 hectares or 66.22% in the inundation area with a depth exceeding 1 meter. These findings demonstrate the effectiveness of embankment in reducing the inundation area without any overtopping incidents.

**KEYWORDS** Flood Management; Estuary Protection; Embankment; Hydrodynamic; HEC-RAS 2D

© The Author(s) 2023. This article is distributed under a Creative Commons Attribution-ShareAlike 4.0 International license.

### 1 INTRODUCTION

Jakarta has always experienced significant challenges in terms of flood management due to its direct adjacency to the sea. The topography and hydrological characteristics of the coastal area make it susceptible to three types of flooding, namely pluvial, fluvial, and coastal flooding. In response, the Indonesian government has implemented various master plans since early 1973, in collaboration with the Netherlands Engineering Consultant (Nedeco), to address flooding issue in Jakarta. Therefore, the most recent and comprehensive flood management master plan is the National Capital Integrated Coastal Development (NCICD) project. The NCICD project entails a series of ini-

tiatives to manage flood in Jakarta effectively. It involves the construction of a 36-kilometre-long seawall along the coast of Jakarta, as well as the implementation of river embankment spanning a total length of 100 kilometres. Among the strategically planned locations for intervention is estuary of Cengkareng Drain.

Similar to most of the Jakarta Coast, Cengkareng Drain estuary consists of settlement and industrial areas. Therefore, the damage caused by flooding will result in huge losses. A previous research by Purnama et al. (2015) conducted in Penjaringan Sub-District showed that economic losses from coastal flooding alone ranged from 424 billion to

4.76 trillion IDR.

Most of the northern part of Cengkareng Drain estuary is located below the mean sea level, as shown in Figure 1. This vulnerable positioning indicates that the area is susceptible to flooding, as a slight rise in sea level can result in inundation. Furthermore, the potential damage caused by flooding can be considerable, depending on its depth and extent. This led to the construction of embankment to safeguard the region from the risk of flooding and mitigate potential damage. However, the planned embankment must be evaluated to enhance flood management in this area.

Extreme conditions need to be considered when managing flooding in coastal area. According to Pasquier et al. (2019), extreme conditions such as high precipitation and storm surges highlight the importance of comprehensively understanding the implications of compound hazards. This corresponds with the research by Kumbier et al. (2018), that hydrodynamic modelling in estuary environment must simultaneously account for both tide and riverine flooding. This consideration is important to avoid underestimating the risk of flooding in an area, as coinciding hazards can have a more significant impact than separate occurrences. Additionally, accurate mapping of flood extent, vulnerability, and risk play a crucial role in the planning and implementing of interventions in flood-prone areas (Araújo et al., 2021).

This research evaluated the effectiveness of coastal and river embankment under compound hazards conditions. According to Bates et al. (2021), comprehensive modelling of flooding in coastal areas requires the consideration of multiple factors. This research considered extreme conditions of high precipitation, high tides, and waves. The research generated inundation maps to display how embankment will reduce flooding during extreme conditions.

## 2 METHODS

Coastal and river embankment performance assessment was performed using hydrological and hydrodynamic simulations using HEC-HMS and HEC-RAS 2D, respectively. This research incorporated several methods to gather and process data.

### 2.1 Research Area: Cengkareng Drain Estuary, Jakarta

Cengkareng Drain Watershed, which covers an area of 25.58 km<sup>2</sup>, is directly adjacent to Jakarta Bay, spanning from West to North Jakarta. The drainage system of the watershed operates downstream of the Pesanggrahan River, which is one of the thirteen rivers traversing Jakarta. It was first initiated on the 'Masterplan for Drainage and Flood Control of Jakarta' as one of the two connector channels. However, the primary purpose of Cengkareng Drain is to facilitate the discharge of water into Jakarta Bay, thereby preventing flooding in the area.

The topography of Cengkareng Drain Watershed is predominantly flat, which impedes the effective gravity flow of water. Consequently, the frequency of local flooding in the region increased. To address this issue, polder systems were implemented, as shown in Figure 2. Each polder has one or more pumps to control the water level in the polder area. These pumps facilitated water transfer from inside the polder system to the nearest water body, aiding flood control efforts.

### 2.2 Data

This research used various hydrological data sources, including daily rainfall data, the digital 2021 with a 1m resolution acquired from Directorate General of Human Settlements (2021).

The DEM data was employed to define the boundaries of Cengkareng Drain watershed and as terrain data for HEC-RAS 2D simulations. In addition, land use data were obtained through Citra Landsat imagery, which played a crucial role in calculating rainfall runoff and estimating the design flood using the SCS-CN method.

Hydrodynamic data used in this research include sea level data, river water level, wind data, and embankment plan. Sea level data was acquired from both observation (SNVT-PTPIN, 2021a,b,c) and sensor data provided by (UNESCO, 2023). These datasets were combined to analyze tides using the Admiralty method. River water level data obtained from the Ciliwung Cisadane River Basin elevation model (DEM), and land use data. The daily rainfall data from 2003 to 2021 was obtained from

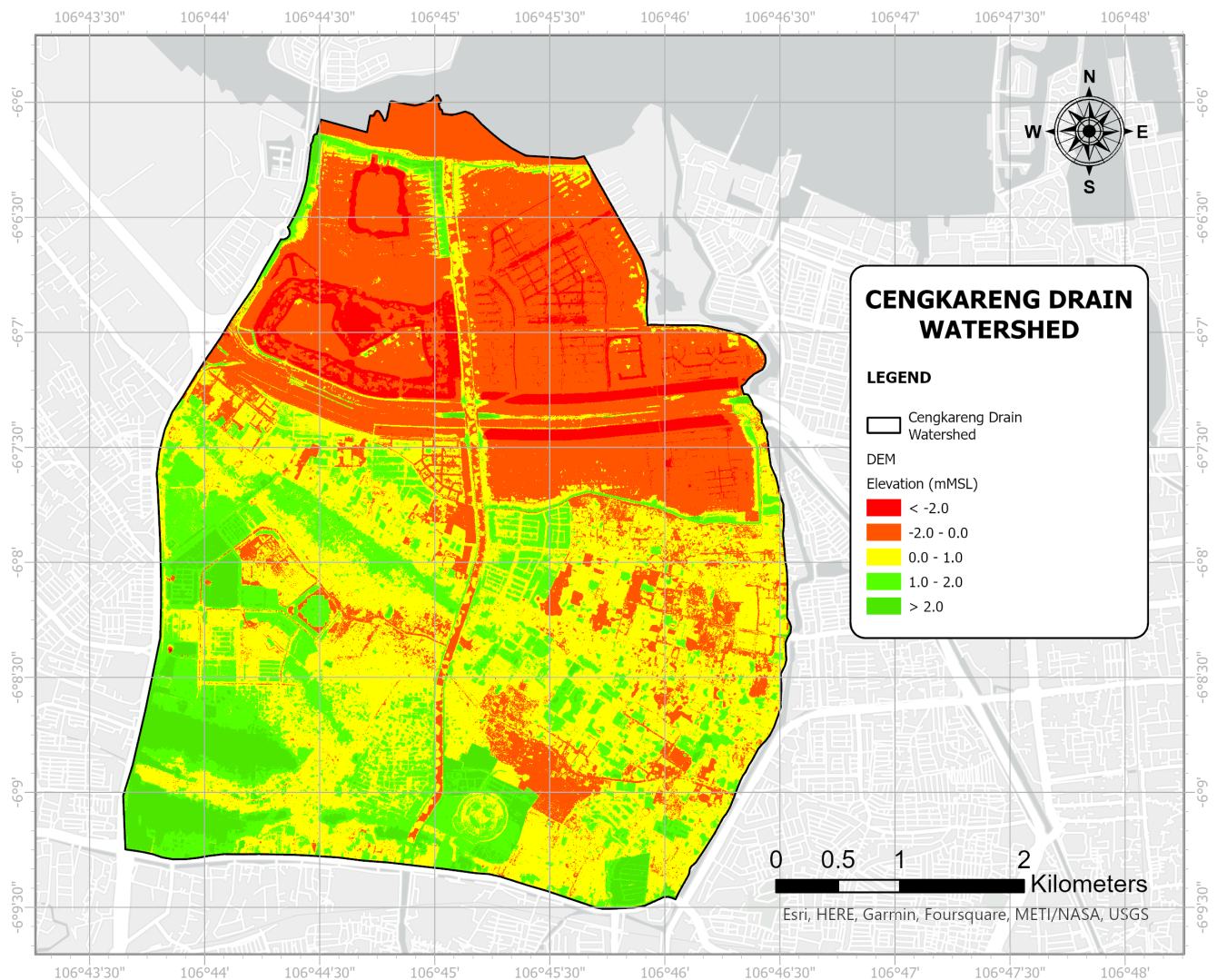


Figure 1 Cengkareng Drain DEM

the Satuan Non-Vertikal Tertentu Pembangunan Terpadu Pesisir Ibukota Negara (SNVT-PTPIN, 2021*a,b,c*). This data was essential for determining the maximum daily precipitation throughout the year and calculating design rainfall. DEM data was gathered from the Directorate General of Human Settlement. Meanwhile, the DEM was LIDAR from Ciliwung Cisadane River Basin Development Agency (2021) were available from 2019 to 2021 and used to calculate river discharge. Wind data from SNVT-PTPIN (2021*a,b,c*) from 2011 to 2020 were used to determine design wave height. Embankment data acquired from SNVT PTPIN provided information on the top elevation of embankment, which is crucial for accurate modelling in HEC-RAS 2D simulations.

### 2.3 Hydrology Model: SCS-CN Method

HEC-HMS software, developed by the US Army Corps of Engineers, simulates precipitation and runoff processes within a watershed. This software offers a range of methods that can be tailored to specific watershed locations and conditions. For high-density urban areas such as Cengkareng Drain, the kinematic wave routing method and SCS-CN are considered suitable.

According to Nasjono et al. (2018), SCS-CN Method is a commonly used empirical approach to calculate direct runoff from precipitation. This method provides a means to understand the relationship between land use characteristics and runoff. It allows for integrating various catchment area characteristics to determine runoff po-

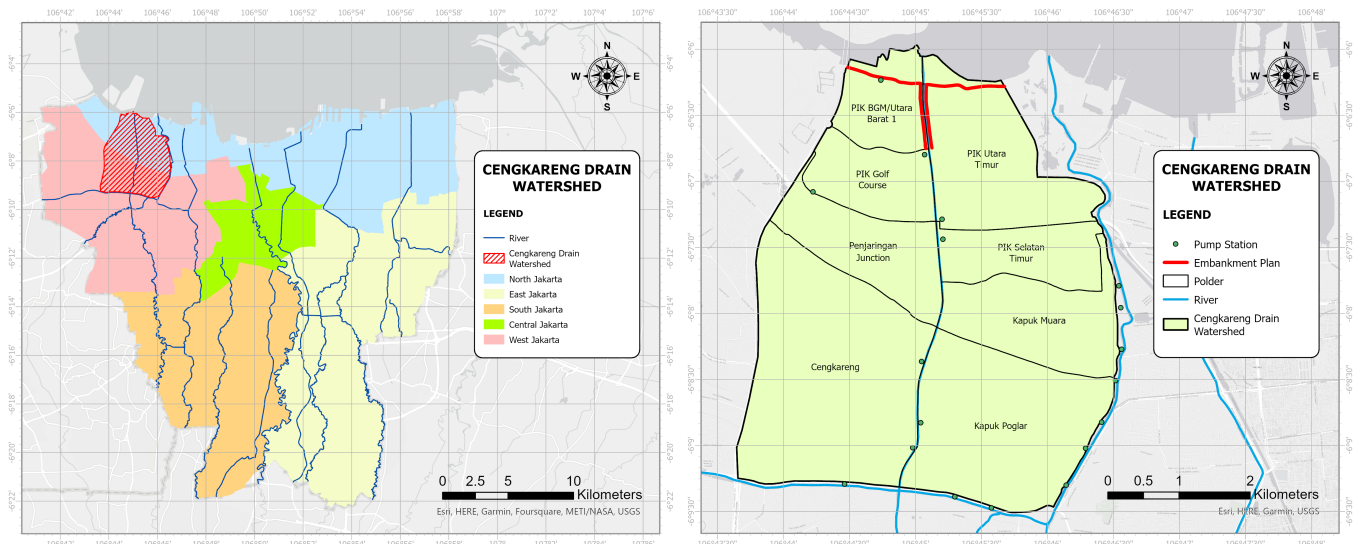


Figure 2 Research area: Cengkareng Drain estuary, Jakarta)

tential. The CN value, a key parameter in the SCS-CN method, is closely associated with the antecedent moisture conditions (AMC), which reflects the moisture content of the soil. The CN value varies depending on the soil conditions. This research assumes that the soil conditions is AMC II representing an average moisture content. Based on research by Chow et al. (1988), the following are the equations used in the SCS-CN method:

$$P_e = \frac{(P - I_a)^2}{P - I_a + S} \tag{1}$$

$$S = \frac{25400}{CN} - 254 \tag{2}$$

where P, P<sub>e</sub>, I<sub>a</sub>, S and CN denote the precipitation (mm), direct runoff (mm), initial abstraction (mm), maximum retention potential (mm), and curve number, respectively. The basic assumption of this method is that runoff occurred after the initial abstraction was fulfilled. This abstraction comprises interceptions, surface storage, and infiltration. Retention potential is a parameter dependent on the catchment's land use. According to the Soil Conservation Service, retention is a function of CN, a relative measure of retention based on land use with a value between 0 and 100. The value itself is determined based on the soil type and previous moisture conditions (AMC).

Rainfall duration is assumed to be 6 hours long and distributed as the alternating block method to de-

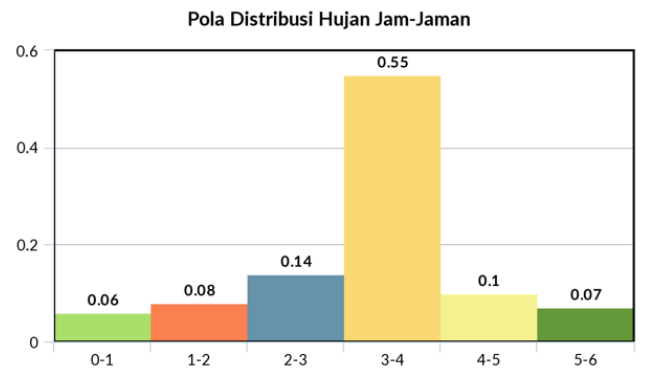


Figure 3 Rainfall pattern for 6-hour duration

velop a hyetograph from the incremental precipitation values. The rainfall pattern is shown in Figure 3.

### 2.4 Sea Level

According to Surinati (2007), tides are a visible natural occurrence in the sea characterized by the vertical movement of seawater mass, ranging from the surface to the deepest parts of the seabed. These ocean tides are primarily caused by gravitational forces and play a crucial role in modelling extreme conditions within estuary. Furthermore, Araújo et al. (2021) stated that high tides are important to consider in modelling coastal flooding.

The admiralty and Least Square methods are commonly used to calculate important sea levels such as LLWL, MSL, and HHWL. One of the distinguishing factors between these two methods is the

length of data needed for their application. The Admiralty method requires a shorter data length, typically 15 or 29 days, while the Least Square method needs a longer data set. Previous research by 'Amalina et al. (2019) examined the differences between the Admiralty and Least Square methods. The results indicated that both methods were relatively reliable and demonstrated only slight disparities. This research used the Admiralty method, which requires shorter data than the Least Square method. The HHWL value, determined using the Admiralty method, will serve as the extreme downstream boundary conditions.

Another factor to be considered is the design wave, estimated from wind data statistically on the assumption that local winds generate the waves. Fetch and wind speed are the parameters used for calculating the significant wave height and period. The formulas are as follows:

$$H_{m0} = 5.112 \cdot 10^{-4} U_A F^{1/2} \quad (3)$$

$$T_o = 6.238 \cdot 10^{-2} (U_A F)^{0.33} \quad (4)$$

where  $H_{m0}$ ,  $T_o$ ,  $U_A$  and  $F$  denote the significant wave height (m), peak period of a wave on the wave spectrum (s), wind stress factor ( $\text{m s}^{-1}$ ), and fetch effective (km), respectively. The design wave can be acquired using Gumbel and Weibull distributions. According to Szymtkiewicz et al. (2018), these distributions are commonly used as they provide agreeable arguments and probability in extreme events. Therefore, the design wave was used as a downstream boundary along with HHWL to represent the coinciding event.

## 2.5 Hydrodynamic Model: HEC-RAS 2D

HEC-RAS, another software developed by the US Army Corps of Engineers, is used for modelling the extent and depth of inundation. Accurate terrain data is needed to employ the two-dimensional model effectively. An open-source DEMNAS combined with bathymetry data (BATNAS) is recommended in this case. However, using higher-resolution terrain data such as LIDAR is much preferable. This is because, as inundation is calculated numerically, the terrain data used in the model plays an important role in making sure that the result depicts the existing conditions.

Flood events were simulated in HEC-RAS using the Saint-Venant equations under unsteady flow conditions. This model applied Saint-Venant equations for both conservation of mass and momentum as follows:

$$\frac{\delta h}{\delta t} + \frac{\delta(hu)}{\delta x} + \frac{\delta(hv)}{\delta y} = q \quad (5)$$

$$\frac{\delta u}{\delta t} + U \frac{\delta u}{\delta x} + V \frac{\delta v}{\delta y} - f_c v = -g \frac{\delta Z_s}{\delta x} +$$

$$\frac{1}{h} \frac{\delta}{\delta x} (V_{t,xx} h \frac{\delta u}{\delta x}) + \frac{1}{h} \frac{\delta}{\delta y} (V_{t,yy} h \frac{\delta u}{\delta y}) - \frac{\tau_{b,x}}{\rho R} + \frac{\tau_{s,x}}{\rho h} \quad (6)$$

$$\frac{\delta v}{\delta t} + U \frac{\delta v}{\delta x} + V \frac{\delta v}{\delta y} - f_c u = -g \frac{\delta Z_s}{\delta y} +$$

$$\frac{1}{h} \frac{\delta}{\delta x} (V_{t,xx} h \frac{\delta v}{\delta x}) + \frac{1}{h} \frac{\delta}{\delta y} (V_{t,yy} h \frac{\delta v}{\delta y}) - \frac{\tau_{b,y}}{\rho R} + \frac{\tau_{s,y}}{\rho h} \quad (7)$$

where  $h$ ,  $t$ ,  $g$ ,  $z_s$ ,  $\rho$ ,  $R$ , and  $f_c$  denote water depth (m), time (s), gravitational acceleration ( $\text{m s}^{-2}$ ), water elevation (m), density ( $\text{kg m}^{-3}$ ), hydraulic radius (m), and Coriolis parameter ( $\text{rad s}^{-1}$ ), respectively. Furthermore,  $u$  and  $v$  are specific flow in both  $x$  and  $y$  directions ( $\text{m}^2 \text{s}^{-1}$ ),  $v_{t,xx}$  and  $v_{t,yy}$  are horizontal eddy viscosity coefficient,  $\tau_{b,x}$  and  $\tau_{b,y}$  denote the components of the effective shear stress ( $\text{N m}^{-2}$ ),  $\tau_{s,x}$  and  $\tau_{s,y}$  are component of the surface wind shear stress ( $\text{N m}^{-2}$ ).

## 2.6 Spearman's $\rho$ Correlation

According to Hiben et al. (2022), Spearman  $\rho$  Correlation is a nonparametric test exhibiting uniform power for linear and nonlinear trends. The test assumes that all data points are independent and identically distributed under the null hypothesis ( $H_0$ ). On the other hand, the alternative hypothesis ( $H_1$ ) suggests an increasing or decreasing trend. The parameters are computed as follows:

$$D = 1 - \frac{6 \sum_{i=1}^n (R_i - i)^2}{n(n^2 - 1)} \quad (8)$$

$$\rho = D \sqrt{\frac{n-2}{1-D^2}} \quad (9)$$

where  $D$  is the difference between the ranks of corresponding variables,  $R_i$  is the rank of  $i^{\text{th}}$  observation,  $n$  is the data length, and  $\rho$  is the Spearman rank correlation. The interpretation of  $\rho$  is shown in Table 1.

Table 1. Strength of Correlation (Fowler et al., 1998)

Value of $\rho$	Meaning
$\pm 0.00$ to $\pm 0.19$	A very weak correlation
$\pm 0.20$ to $\pm 0.39$	A weak correlation
$\pm 0.40$ to $\pm 0.69$	A moderate correlation
$\pm 0.70$ to $\pm 0.89$	A strong correlation
$\pm 0.90$ to $\pm 1.00$	A very strong correlation

In order to determine whether the hypothesis would be accepted, it is crucial to calculate the p-value. The p-value represents the significance level of the correlation observed in the data. The implications of rejecting the null hypothesis ( $H_0$ ) varies based on the specific p-value obtained, as shown in Table 2.

Table 2. P-value and Evidence for Rejecting  $H_0$  (Fowler et al., 1998)

P-value	Evidence for Rejecting $H_0$
$> 0.10$	Very weak to none
$0.05 - 0.10$	Weak
$0.01 - 0.05$	Strong
$< 0.01$	Very strong

## 2.7 Model Performance Evaluation

There are several methods for evaluating simulation quality and reliability, such as Correlation Coefficient (R), Nash-Sutcliffe Efficiency (NSE), Percentage Bias (PBIAS), and Peak Flow Criterion (PFC) (Anh et al., 2022). The present research specifically employed the NSE and PBIAS methods. The following are the equations (Ji et al., 2020) and ratings for the respective methods.

$$NSE = 1 - \frac{\sum_{i=1}^n (R_{0,i} - R_{m,i})^2}{\sum_{i=1}^n (R_{0,i} - R_0)^2} \quad (10)$$

$$PBIAS = \frac{\sum_{i=1}^n (R_{0,i} - R_{m,i})^2}{\sum_{i=1}^n (R_{0,i})} \times 100\% \quad (11)$$

Table 3. Model Performance Rating (Anh et al., 2022)

Performance	NSE	PBIAS
Very Good	$0.75 < NSE \leq 1.00$	$PBIAS < \pm 10$
Good	$0.65 < NSE \leq 0.75$	$\pm 10 < PBIAS < \pm 15$
Satisfactory	$0.50 < NSE \leq 0.65$	$\pm 15 < PBIAS < \pm 25$
Unsatisfactory	$NSE \leq 0.50$	$PBIAS \geq \pm 25$

## 3 RESULTS

### 3.1 Parameter and Scenario Definition

Prior to conducting the simulations, it is crucial to determine the parameters and scenarios. Each scenario should accurately represent Cengkareng Drain system under various conditions.

This research used two scenarios, as shown in Table 4. Scenario A simulated the existing conditions, with the base year set as 2020. On the other hand, Scenario B represented where embankment had been constructed under existing conditions.

The parameters used are embankment, upstream, and downstream boundaries. Both scenarios use river discharge and the 100-year design flood as the upstream boundaries. Meanwhile, the downstream boundaries comprise the HHWL (Highest High-Water Level) and the 100-year design wave. The key difference between both scenarios is the presence or absence of embankment. The elevation of embankment is +4.00 mLWS or +3.40 mMLS, as stated in the NCICD embankment plan (PT Aditya Engineering Consultant, 2020).

Table 4. Simulation Scenarios

Scenario	Embankment	Upstream Boundary	Downstream Boundary
A	-	River Discharge	HHWL and 100-year Design Wave
B	v	and 100-year Design Flood	

### 3.2 Calibration and Validation

The calibration and validation process of the model is a critical step in ensuring the reliability of its result. While the ideal approach would have involved using past inundation area data, it was not feasible due to its unavailability and lack of

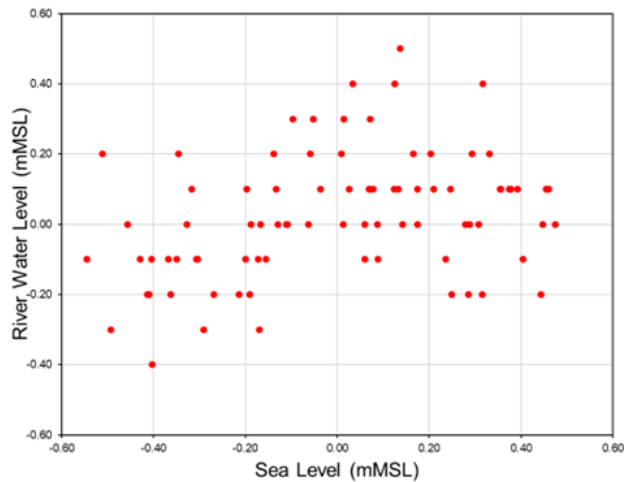


Figure 4 Comparison of sea level and river water level

accuracy. As a result, there is a potential for the modelled inundation to be either over or underestimated. The calibration and validation were then carried out using observed river water level data from Cengkareng Drain sluice gate.

River water level data was recorded at irregular intervals every six to twelve hours, which was insufficient for direct comparison with the model. However, it was also observed that tides greatly influence these readings. This relationship between sea and river water levels is shown in Figure 4. Using Spearman  $\rho$  Correlation, the coefficient of  $\rho$  and p-value are 0.3152 and 0.00294, respectively. Statistically, this indicates a significant correlation between the two datasets. The p-value is less than 0.05 (5%) depicts that the correlation is not just by chance (Sutjiningsih et al., 2021). Adjusting river water level data to align with the sea level readings becomes viable. Since sea level data is recorded at more frequent intervals, typically every minute, it offers higher accuracy. Instead of solely relying on river water level readings, the calibration process will incorporate river and sea level data.

The calibration and validation of the model were performed using data from the event that occurred in February 2020. The parameter being calibrated was the Manning roughness coefficient of river channel. Upon completion of the calibration process, the selected value for the Manning roughness coefficient was determined to be 0.017. Figure 5 visually compares the modelled river water level after calibration and the observed data. In this research, the NSE and PBIAS methods were used to

Table 5. Simulation Evaluation

Methods	Value
NSE	0.80
PBIAS	-1.33%

evaluate performance of the simulation model, as shown in Table 5. The results indicate that the NSE and PBIAS values exhibited a high level of performance. Consequently, the model is deemed suitable for conducting additional simulations.

Certain factors were identified as significant contributors to model performance during the calibration and validation processes. Two such factors were the presence of a seasonal signal in river discharge data and the daily recording of precipitation data. These factors have been found to pose challenges that can affect the accuracy of modelling results, particularly in simulating hourly flow hydrographs and predicting flood. This shows the importance of having precipitation recorded continuously.

### 3.3 Hydrology Simulation

HEC-HMS is used to conduct hydrology simulation of the Cengkareng Drain Watershed. The model configuration used for this simulation is shown in Figure 6. The model defined each of the sub-watersheds, junctions, and reaches.

The SCS-CN method was used to estimate the parameter. Meanwhile, the methods for the transform parameter are SCS unit hydrograph and kinematic wave for each sub-watershed and reach, respectively. In using each of these methods, several input parameters must be considered.

The observed precipitation data from the rain gauge at Cengkareng Drain was analyzed, leading to the conclusion that it follows a Type 3 Log Pearson distribution. This distribution was then used to calculate design rainfall for various return periods, as shown in Figure 7. Cengkareng Drain was designed to accommodate a 100-year return period flood. Consequently, a 100-year return period rainfall of 206.97 mm was selected. It is necessary to apply a reduction factor to the design rainfall due to the use of only one rain gauge. A reduction factor of 0.88 was employed to adjust the design

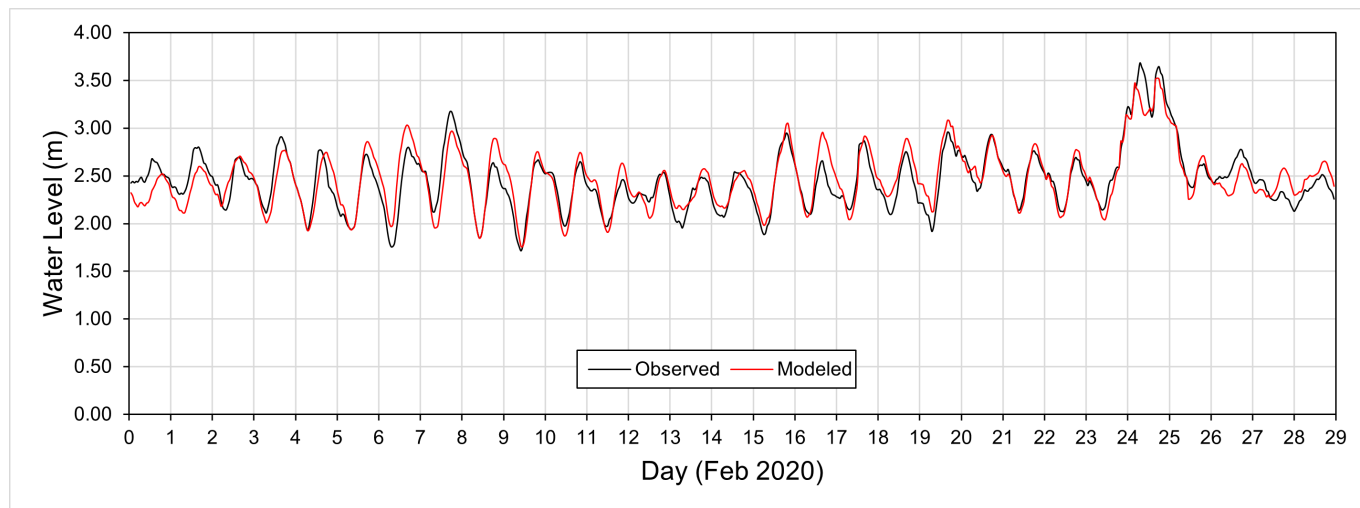


Figure 5 Comparison of observed and modeled water levels in February 2020

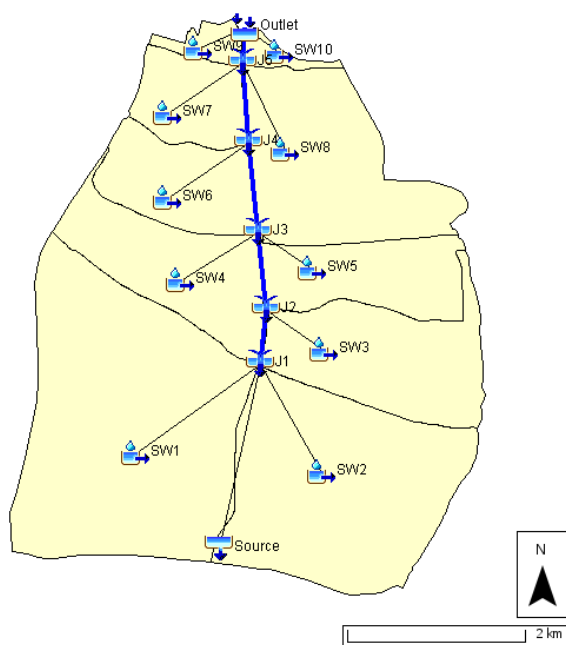


Figure 6 Cengkareng Drain watershed basin model

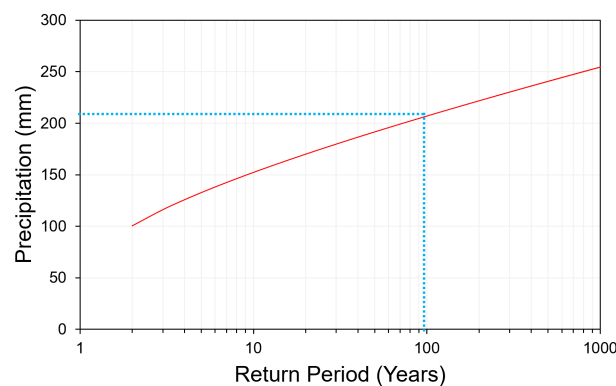


Figure 7 Design rainfall for various return periods

rainfall, resulting in a value of 182.13 mm.

During the design flood simulation using HEC-HMS, two crucial parameters were required, namely the impervious cover percentage and the CN (Curve Number) value for the watershed. The impervious cover encompasses both settlements and water bodies within the watershed area. Meanwhile, the CN value varies for each land use. Both parameters were obtained from the land use map shown in Figure 8.

The simulation results shown in Figure 9 depict a flow hydrograph showcasing the series of dis-

charge values at each junction and the outlet within the watershed. The peak discharge at the outlet occurs 7 hours after the onset of precipitation and reaches a magnitude of  $160.9 \text{ m}^3 \text{ s}^{-1}$ . In order to determine the precise river discharge, the baseflow needs to be added to the peak discharge value. Furthermore, the flood is expected to subside after 38 hours.

### 3.4 Sea Level

The analysis of sea level elevation was conducted using the Admiralty method. Hourly observed sea level measurements obtained from February 1<sup>st</sup> to 29<sup>th</sup>, 2020, were used for this investigation. The results provided significant sea level elevations, namely MSL, HHWL, LLWL, MHWL, and MLWL, with the following values +0.625 m, +1.223 m, -0.136 m, +0.799 m, and +0.560 m, respectively. These important elevations were then

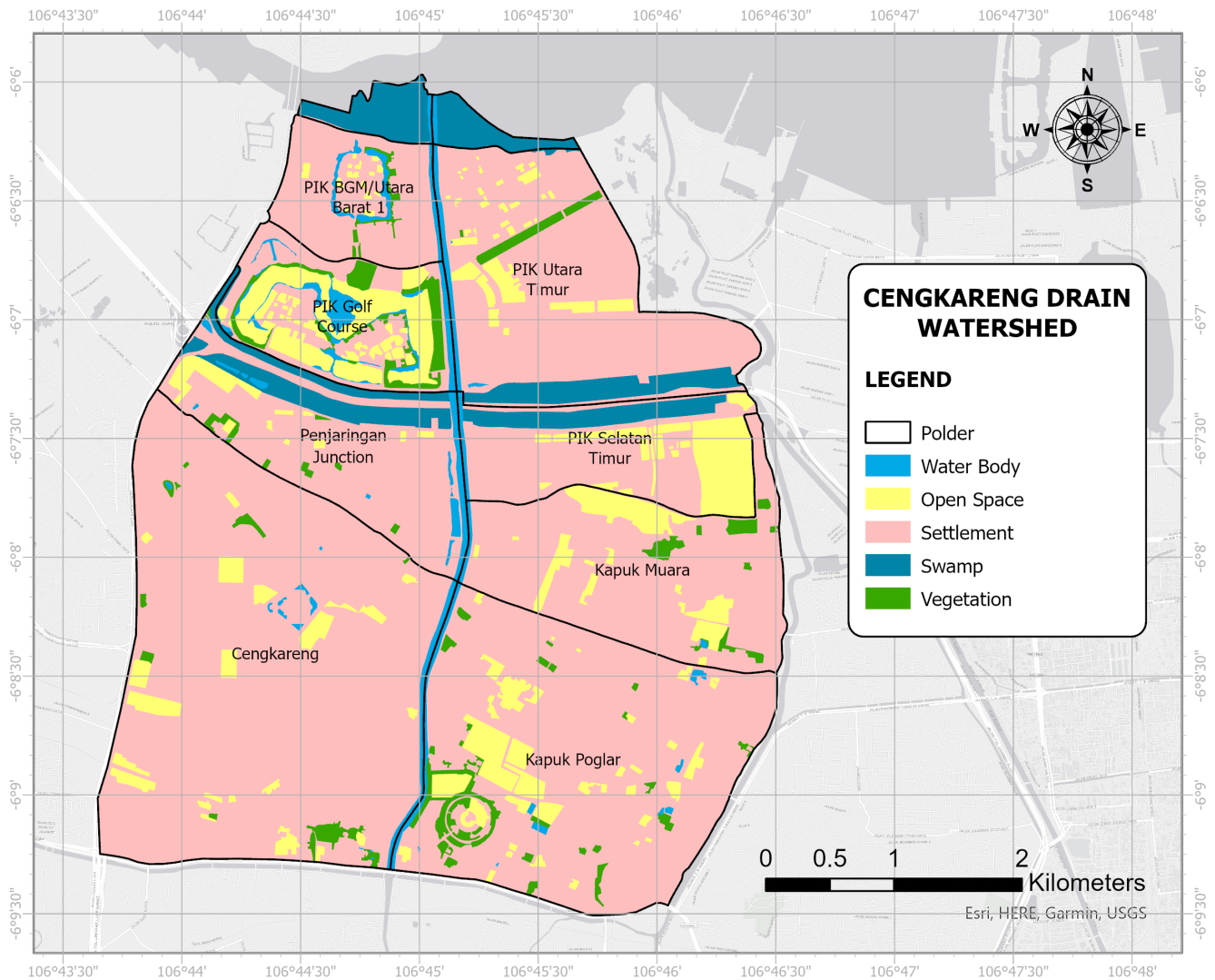


Figure 8 Cengkareng Drain land use

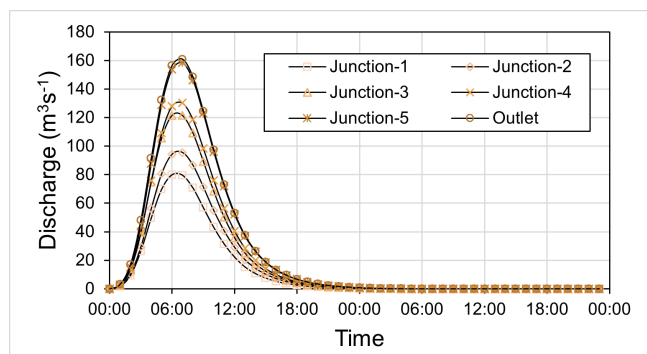


Figure 9 Flow hydrograph on junctions and outlet

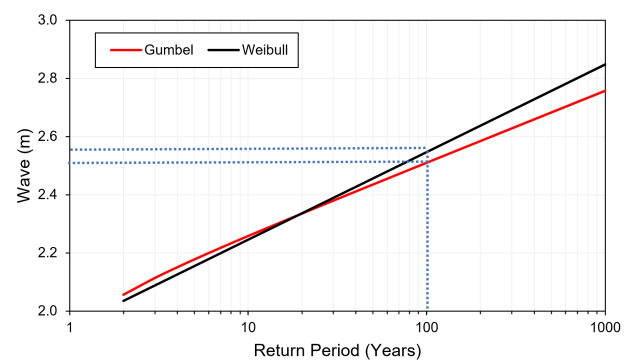


Figure 10 Design wave for various return periods

adjusted with reference to the MSL to facilitate further analysis and comparisons. The adjusted values denoted as +0.000 mMSL, +0.598 mMSL, -0.489 mMSL, +0.174 mMSL, and -0.065 mMSL provide a relative reference to the Mean Sea Level. This adjustment allows for easier interpretation

and enables subsequent analysis of the sea level data. The design of the NCICD embankment includes the consideration of a 100-year return period wave. In order to ensure the effectiveness of

embankment, the simulation takes this factor into account. The Gumbel and Weibull distributions were used to analyzed and determine the design wave, with the result shown in Figure 10. These distributions play a crucial role in understanding and modelling the characteristics of the design wave for embankment.

The 100-year return period design wave was analyzed using the Weibull distribution resulting in 2.547 m. This value is higher than that of the Gumbel distribution. Therefore, it was used to establish the boundary for hydrodynamic simulation. This selection ensures that the simulation adequately incorporates the higher magnitude of the design wave, as indicated by the Weibull distribution analysis.

### 3.5 Hydrodynamic Simulation

Hydrodynamic model was developed using HEC-RAS 2D, incorporating terrain and geometric data. The terrain data was adjusted to align with the MSL to be consistent with other information used in the research. The geometry data includes Cengkareng Drain Watershed represented as a 2D Flow Area, along with the inclusion of river and existing pumps. This comprehensive representation accounts for multiple polders within the area, ensuring an accurate simulation of flow dynamics in the model.

Hydrodynamic model also used two boundary conditions, namely flow and stage hydrographs, for the upstream and downstream boundaries, respectively. In order to determine the stage hydrograph, the 100-year design wave was added to the HHWL elevation. The boundaries were selected to depict extreme conditions. Figure 11 shows hydrodynamic model used, clearly representing its configuration and components.

HEC-RAS two-dimensional analysis generated an inundation map and depth results shown in Figure 12. The result predicted that a total area of 1212.37 ha in scenario A would be flooded. The northern part of the watershed would experience inundation with depths exceeding 1 m. For scenario B, the total inundation area was 1111.22 ha. In scenario A, the occurrence of extreme events in the model resulted in the overtopping of embankment. Overtopping occurs when the water level

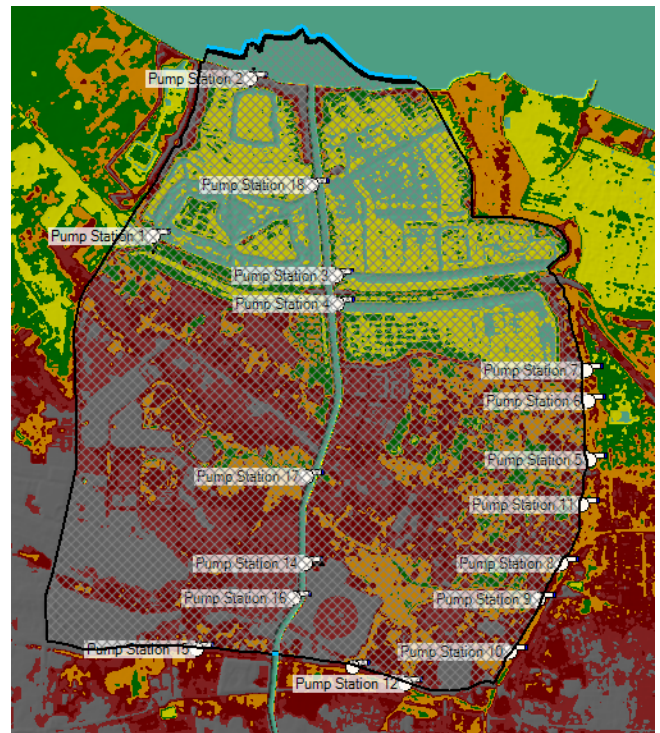


Figure 11 Cengkareng Drain watershed hydrodynamic model

in both river and sea exceeds embankment height. Furthermore, in the modelled scenario, the precipitation that coincides with tides and waves exacerbates the extent of inundation.

NCICD embankment plan along the research area has an elevation of +3.40 mMSL. This value is used for scenario B to replace the previously existing embankment height. Figure 12 showed that embankment was not exceeded, as the maximum water level influenced by the HHWL and design wave was +3.145 mMSL.

The implementation of embankment reduced the total inundation area by 101.15 ha, as shown in Table 6. Inundation with a depth of more than 1 m is reduced by 86.49 ha or 66.22%. In a densely populated area such as Cengkareng Drain estuary, reduction of inundation would also significantly reduce the possible damage to property and infrastructure.

## 4 DISCUSSION

Previous research has reported the importance of establishing a consistent datum. According to Breili et al. (2020), discrepancies between tides and DEM data tend to introduce errors that could

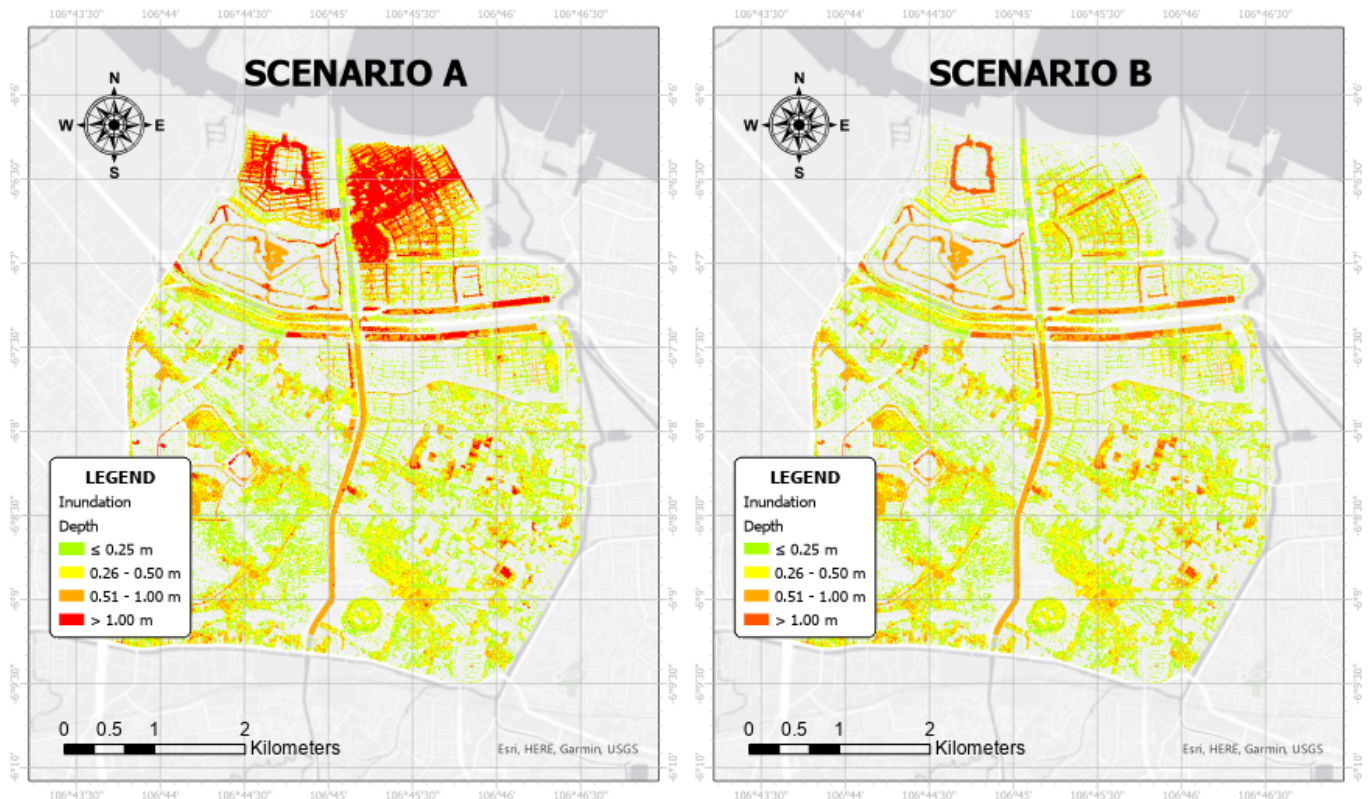


Figure 12 Inundation maps for each scenario

Table 6. Inundation Areas for Each Depth Classification and Scenario

Depth (m)	Area (ha)	
	Scenario A	Scenario B
≤0.25	484.31	518.42
0.26-0.50	333.19	341.65
0.51-1.00	264.26	207.03
>1.00	130.61	44.12
<b>Total</b>	<b>1212.37</b>	<b>1111.22</b>

affect the calculated inundation area. Although these errors may not always be significant, they could become more pronounced when modelling areas with great slopes, such as estuary. In this case, using a consistent datum for recording is best.

The findings from preliminary research and observations have reported that extreme conditions may not always be a coincidence. Therefore, the result of the simulation tends to be overestimated. It is essential to incorporate these extreme conditions in the simulations, as there is a probability for them to occur simultaneously. Further analysis is needed to support decision-making in selecting

the appropriate capacities and dimensions of the structure.

The simulation results showed that inundation with a depth of more than 1 m can be reduced to approximately 66.22%. However, the precision of this value was affected by the limitations of the LIDAR data, which only captures the elevation of objects. Accuracy could be improved by further refining the data through field surveys and adjustments. These findings highlighted the successful performance of embankment in reducing flooding under compound hazards in the current conditions. It does not mean that raising the top of embankment would resolve all the problems related to Cengkareng Drain. This research is focused on analyzing the existing conditions and does not encompass an assessment of possible future hazards.

There are also some limitations regarding hydrodynamic model that needs to be addressed. HEC-RAS, primarily designed for simulating river or channel flows, may not accurately represent the intricate tidal interactions in estuary. Moreover, the lack of previous inundation data prevented the calibration of HEC-RAS model. There is a possibility that the modelled inundation is underesti-

mated or overestimated due to these inherent limitations.

Local subsidence is one of the most concerning factors in the research location. The efficiency of embankment could be compromised due to the sinking of the structures caused by land subsidence, can lead to structural deformation, potential breaches, or failures. According to Fiaschi and Wdowinski (2020), land subsidence is one of the main factors contributing to coastal flooding. Previous research conducted by Abidin et al. (2008) has also analyzed the characteristics of land subsidence in Jakarta, revealing an estimated annual subsidence rate of 1 to 10 cm year<sup>-1</sup>. Even though the rate of land subsidence is not constant, its significant magnitude raises concerns. Land subsidence is an important factor that must be considered in future evaluations.

In the light of global climate change, it is imperative to consider the potential impact of sea level rise. This is crucial as sea level rise increases the hydraulic load on coastal embankment and can cause water levels to exceed previous design levels. Triana and Wahyudi (2020) stated that rising sea levels pose a heightened coastal flooding risk. According to NOAA, there was an average sea level rise of approximately  $4.5 \pm 0.4$  mm year<sup>-1</sup> between 1992 and 2022. While MSL may not consistently rise throughout the years, the overall trend is unmistakable. Mayo and Lin (2022) stated that the frequency and severity of flood hazards are expected to increase significantly due to sea level rise by the end of this century.

The combination of land subsidence and sea level rise poses a significant threat to embankment structures. When the structures sink, and the water level surpasses the design level, the vulnerability to overtopping increases, resulting in a heightened risk of estuary flooding. Given that a considerable portion of the northern area of Cengkareng Drain is already situated below the mean sea level, this combination further exacerbates the potential for severe risk and losses.

In order to assess the long-term viability of embankment in mitigating compound hazards, it is essential to evaluate their performance under future conditions that account for land subsidence and sea level rise. Furthermore, a thorough analysis of the effectiveness of the pumps in the polder

system in terms of reducing the inundation duration and area is necessary for future development. Depending on the results, additional pumps need to be installed.

The findings of this research have significant implications for various applications, such as identifying high-risk areas and conducting risk assessments. The information on potential inundation depth and area can aid in determining suitable investments for flood risk reduction through cost-benefit analyses. Furthermore, these results are crucial for future development plans, policy planning, and efforts to enhance coastal resilience.

## 5 CONCLUSION

In conclusion, this research used HEC-RAS 2D to assess performance of coastal and river embankment under different sources of flooding. The boundary conditions included extreme scenarios involving high precipitation, tides, and waves. The results showed that the structures exhibited improved performance, reducing the inundation area by 101.15 hectares.

Inundation in areas with more than 1m depth occurs due to the overtopping of existing embankment. NCICD coastal and river embankment elevation can prevent overtopping, as the elevation is higher than extreme water level conditions. As a result, the inundation area with depths of 1 meter was significantly reduced by 86.49 hectares or 66.22%.

The simulations provided valuable insights into the effectiveness of the planned embankment in protecting Cengkareng Drain estuary from compound hazards. It highlighted the importance of considering multiple hazards when modelling coastal areas. Meanwhile, the remaining inundation should be pumped to the nearest water body. Future investigations should focus on assessing the capacity of the existing pumps to reduce inundation in these areas effectively.

Due to the use of HEC-RAS, hydrodynamic model may not be able to depict all the complex tidal interactions in estuary. The reason is that it was not initially designed to model coastal areas. Therefore, future research should consider using a more specialized model to account for those processes.

The current evaluation indicates that the planned embankment has successfully reduced flooding in the area. However, it is essential to conduct a future assessment to determine the long-term performance of these structures in the face of local land subsidence and anticipated sea level rise. This evaluation helps identify potential issues and enable the implementation of necessary countermeasures and additional coastal protection approaches.

The two-dimensional simulation revealed that the planned embankment effectively protects Cengkareng Drain estuary. These findings help to support embankment plans in other locations and enhance coastal resilience. It can also be used to conduct risk assessments and determine appropriate investments in flood risk reduction. In the future, it would be important to assess performance of structures while considering other local issues.

#### DISCLAIMER

The authors declare no conflict of interest.

#### AVAILABILITY OF DATA AND MATERIALS

All data are available from the author.

#### ACKNOWLEDGMENTS

The authors are grateful to Universitas Indonesia for their assistance in this research. The authors are also grateful to the Directorate General of Human Settlement and SNVT PTPIN for providing data and all the reviewers for their input.

#### REFERENCES

Abidin, H., Andreas, H., Djaja, R., Darmawan, D. and Gamal, M. (2008), 'Land subsidence characteristics of jakarta between 1997 and 2005, as estimated using gps surveys', *GPS Solutions* **12**(1), 23–32.

Anh, T., Huu, X., Tuong, V. and Tai, L. (2022), 'Application of hec-hms model and satellite precipitation products to restore runoff in laigiang river basin in vietnam', *Indonesian Journal of Geography* **54**(1), 1–10.

Araújo, P., Amaro, V., Aguiar, L., Lima, C.

and Lopes, A. (2021), 'Tidal flood area mapping fronts climate change scenarios: Case study in a tropical estuary in the brazilian semi-arid region', *Natural Hazards and Earth System Sciences* **21**(11), 3353–3366.

Bates, P., Quinn, N., Sampson, C., Smith, A., Wing, O., Sosa, J., Savage, J., Olcese, G., Neal, J., Schumann, G., Giustarini, L., Coxon, G., Porter, J., Amodeo, M., Chu, Z., Lewis-Gruss, S., Freeman, N., Houser, T., Delgado, M., Hamidi, A., Bolliger, I., McCusker, K., Emanuel, K., Ferreira, C., Khalid, A., Haigh, I., Couasnon, A., Kopp, R., Hsiang, E. and Krajewski, W. (2021), 'Combined modelling of us fluvial, pluvial, and coastal flood hazard under current and future climates', *Water Resources Research* **57**(2), 1–29.

Breili, K., James Ross Simpson, M., Klokervold, E. and Roaldsdotter Ravndal, O. (2020), 'High-accuracy coastal flood mapping for norway using lidar data', *Natural Hazards and Earth System Sciences* **20**(2), 673–694.

Chow, V., Maidment, D. and Mays, L. (1988), *Applied Hydrology*, xiii edn, McGraw-Hill.

Ciliwung Cisadane River Basin Development Agency (2021), 'Data Pembacaan Tinggi Muka Air Cengkareng Drain Tahun 2019 - 2021'. Jakarta.

Directorate General of Human Settlements (2021), 'Peta lidar dki jakarta', Jakarta.

Fiaschi, S. and Wdowinski, S. (2020), 'Local land subsidence in miami beach (fl) and norfolk (va) and its contribution to flooding hazard in coastal communities along the u.s. atlantic coast', *Ocean and Coastal Management* **187**, 105078.

Fowler, J., Cohen, L. and Jarvis, P. (1998), *Practical Statistics for Field Biology*, 2nd edn, John Wiley & Sons, Inc.

Hiben, M., Gebeyehu Awoke, A. and Adugna Ashenafi, A. (2022), 'Hydroclimatic variability, characterization, and long term spacio-temporal trend analysis of the ghba river subbasin, ethiopia', *Advances in Meteorology*.

Ji, X., Li, Y., Luo, X., He, D., Guo, R., Wang, J., Bai, Y., Yue, C. and Liu, C. (2020), 'Evaluation of bias correction methods for aphrodite data to improve hydrologic simulation in a large himalayan basin', *Atmospheric research* **242**, 104964.

- Kumbier, K., Carvalho, R., Vafeidis, A. and Woodroffe, C. (2018), 'Investigating compound flooding in an estuary using hydrodynamic modelling: A case study from the shoalhaven river, australia', *Natural Hazards and Earth System Sciences* **18**(2), 463–477.
- Mayo, T. and Lin, N. (2022), 'Climate change impacts to the coastal flood hazard in the northeastern united states', *Weather and Climate Extremes* **36**, 100453.
- Nasjono, J., Utomo, S., Marawali, U., Debit, P. and Number, S. (2018), 'Keandalan metode soil conservation services-curve number untuk perhitungan debit puncak das manikin', *Jurnal Teknik Sipil* **VII**(2), 183–192.
- Pasquier, U., He, Y., Hooton, S., Goulden, M. and Hiscock, K. (2019), 'An integrated 1d–2d hydraulic modelling approach to assess the sensitivity of a coastal region to compound flooding hazard under climate change', *Natural Hazards* **98**(3), 915–937.
- PT Aditya Engineering Consultant (2020), 'Laporan detail desain pengaman pantai ibukota negara tahap 2', Jakarta.
- Purnama, S., Marfai, M., Anggraini, D. and Cahyadi, A. (2015), 'Estimasi risiko kerugian ekonomi akibat banjir rob menggunakan sistem informasi geografis di kecamatan penjaringan, jakarta utara', *Jurnal SPATIAL Wahana Komunikasi dan Informasi Geografi* **14**(2), 8–13.
- SNVT-PTPIN (2021a), 'Data angin harian tahun 2011 - 2021', Jakarta.
- SNVT-PTPIN (2021b), 'Data curah hujan pch cengkareng drain 2003–2021', Jakarta.
- SNVT-PTPIN (2021c), 'Data pasang surut 4 - 19 oktober 2021', Jakarta.
- Surinati, D. (2007), 'Pasang surut dan energinya', *Oseana* **xxxii**(1), 15–22.
- Sutjiningsih, D., Soeryantono, H., Anggraheni, E. and Saleh, T. (2021), 'The biotic integrity of ciliwung river in west java under multiple urban stressors', *IOP Conference Series: Earth and Environmental Science* **641**(1), 012005.
- Szmytkiewicz, M., Szmytkiewicz, P. and Marcinkowski, T. (2018), 'Comparison of design wave heights determined on the basis of long- and short-term measurement data', *Archives of Hydroengineering and Environmental Mechanics* **65**(2), 123–142.
- Triana, K. and Wahyudi, A. (2020), 'Sea level rise in indonesia: The drivers and the combined impacts from land subsidence', *ASEAN Journal on Science and Technology for Development* **37**(3), 115–121.
- UNESCO (2023), 'Sea level station monitoring facility', <https://www.ioc-sealevelmonitoring.org/>. [Accessed 10 May 2023].
- 'Amalina, A., Atmodjo, W. and Pranowo, W. (2019), 'Karakteristik pasang surut di teluk jakarta berdasarkan data 253 bulan', *Jurnal Riset Jakarta* **12**(1), 25–36.